# Voltammetric study of formic acid oxidation via active chlorine on IrO₂/Ti and RuO₂/Ti electrodes

**Kambiré Ollo [1,*], Pohan Lemeyonouin Aliou Guillaume [2], Sadia Sahi Placide [3], Kouadio Kouakou Etienne [3] and Ouattara Lassiné [3,*]**

[1] UFR Sciences et Technologies, Université de Man, BP 20 Man, Côte d'Ivoire

[2] UFR Sciences Biologiques, Université Peleforo Gon Coulibaly de Korhogo, BP 1328 Korhogo, Côte d'Ivoire

[3] Laboratoire de constitution et réaction de la matière, UFR SSMT, Université Félix Houphouët-Boigny de Cocody, Abidjan, 22 BP 582 Abidjan 22, Côte d'Ivoire

**Abstract**: This work aimed to contribute to the mechanism electrochemical oxidation study of organic compounds on DSA electrodes. To do this, $IrO_2$ and $RuO_2$ electrodes were prepared thermally at 40°C on Titanium substrate. The prepared electrodes were characterized using voltammetric and SEM techniques. The electrochemical measurements in acid media made it possible to show the presence of $IrO_2$ and $RuO_2$ on the surface of the electrode. These electrodes have identical electrocatalytic behaviors both for oxygen evolution and chlorine evolution. The prepared electrodes make it possible to oxidize the organic compounds in an acid media in the absence or in the presence of $Cl^-$. In acidic electrolytes, water molecules produce hydroxyl radicals that contribute to the higher oxides ($RuO_3$ or $IrO_3$) formation. The higher oxides obtained produce $O_2$ and regenerate the active sites of our electrodes. In the electrolytes containing chlorides, higher oxides fix them ($IrO_3(Cl)$ or $RuO_3(Cl)$) in competition with the production of $O_2$. Then $IrO_3(Cl)$ or $RuO_3(Cl)$ reacts with $Cl^-$ to produce $Cl_2$ and regenerate the adsorbed hydroxyl radicals. The higher oxides also react as a mediator in HCOOH oxidation in competition with $O_2$ evolvement. In the electrolytes containing HCOOH and $Cl^-$, the organic pollutant's oxidation occurs indirectly via the hypochlorite ions produced in the solution and on the electrodes. This study showed that the produced OH· and $Cl_2$ in situ are involved in the oxidation of HCOOH.

**Keyswords**: electrode; metallic oxides; oxygen; chlorine; formic acid.

## 1. Introduction

The application of electrochemical technologies to environmental pollution abatement has been the topic of several books [1–6]. The main advantage of these technologies is the ability to mineralize harmful pollutants into simple inorganic compounds such as $H_2O$ or $CO_2$, which are natural for the environment. Generally, the organic pollutants mineralization occurs on the anode surface via the production of hydroxyl radicals [6–8] or/and other oxidants. Thus, anode material plays a crucial part in the electrochemical technologies [9-12].

In recent years, with the introduction of dimensionally stable anodes (DSA) by H. Beer [13], metal oxide electrodes (such as $RuO_2$ and $IrO_2$) have become increasingly technologically important. Major characteristics of these anodes are longer operating lifetime [14] and comparatively low cost [15,16]. Thus, the DSA anodes constitute an important class of stable electrocatalysts [17] mainly used in the chloro-alkali industry [18], in the production of oxygen and hydrogen in water electrolysis, and have received attention wastewater treatment [19]. The main drawback of using DSA is the generation of highly reactive oxidants limited (like hydroxyl radicals), reducing their wastewater treatment efficiencies. Therefore, it is necessary to overcome that limit.

According to the literature [20,21], the generation of highly reactive oxidants might be overcome if DSA is irradiated with UV light. Besides, these anodes have the facility to generate chloro oxidant species ($Cl_2$, HOCl, and OCl) when electrolysis is carried out at chloride-containing medium [1-3]. In several studies, NaCl has been employed as the salt to increase electrolyte [1,3,6]. However, few works have reported organic compounds' mechanism degradation via chloro oxidant species on DSA anodes.

Different voltammetry techniques can be used to study an electrochemical system's response to polarization: linear, cyclic, and square wave voltammetry. Voltammetry is one of the most important electroanalysis techniques [22,23], also used

for the reaction mechanisms determination [24-26]. Its strength lies in the simplicity of implementation and the wealth of information collected for the redox processes study.

For this reason, this work aims to study the oxidation mechanism of synthetic effluent in the presence of different $Cl^-$ concentrations, using DSA anodes. Owing to their high electrocatalytic properties, we used $RuO_2$ and $IrO_2$ as electrodes to study the oxidation of the formic acid in the presence of oxygen ($O_2$) and chlorine ($Cl_2$) evolution by voltammetric measurements. Formic acid was chosen because it is the smallest molecule with the four most common chemical bonds in organic compounds (C−H, C=O, C−O, O−H), making formic acid an ideal model molecule for studying electrooxidation reactions [27].

## 2. Experimental

### 2.1. Preparation of $RuO_2$ (ruthenium oxide) and $IrO_2$ (Iridium oxide) anodes

$RuO_2$ and $IrO_2$ electrodes were prepared by the thermal decomposition method on titanium substrates. The precursor solution is made by the dissolution of $RuCl_3.xH_2O$ (Fluka, 99.98 %) and $H_2IrCl_6.6H_2O$ (Fluka, 99 %) in pure isopropanol (Fluka, 99.5 %). Before the deposition and to ensure maximum adhesion of the coating, the substrate (Titanium) was sandblasted. The precursor was applied by a painting procedure on the titanium (Ti) substrate then put in an oven for 10 minutes at 80°C to allow the solvent evaporation. It is then placed in a furnace at 400°C for 15 minutes to allow the precursor's decomposition. These steps were repeated until the desired mass of the coating is reached. A final decomposition of 1 h was done at 400°C [14, 24-26, 28]. The deposits' loading is around     $(5, 0 \pm 0, 3)$ g/m².

### 2.2. Electrochemical measurements

The electrochemical measurements were performed in a three-electrode cell. The working electrode was $IrO_2$ or $RuO_2$ electrode, the counter electrode was a platinum wire, and the reference electrode was a saturated calomel electrode (SCE). The electrochemical study (potentiodynamic polarization) is carried out using an experimental device composed of an Autolab Potentiostat de ECHOCHEMIE (PGSTAT 20), interfaced with a computer. To overcome the potential ohmic drop, the reference electrode was mounted in a luggin capillary and placed close to the working electrode by a distance of 1 mm. The apparent exposed area of the working electrode was 1 cm².

The chemicals used for the electrochemical study are $HClO_4$ (Suprapur Merck, 70 %), NaCl (Fluka, 99 %),

and HCOOH (Fluka, 98 %). All solutions were prepared with distilled water, and the experiments were carried out at room temperature at 25°C.

To decrease the potential ohmic drop's contribution, the reference electrode was mounted in a luggin capillary and placed close to the working electrode by a distance of 1 mm. The ohmic drop is known to increase the Tafel slope value, and careful attention was paid to it during the experiment. To reduce the residual ohmic drop, the polarization curve should be corrected according to the method described elsewhere [29-32]. A brief description of the correction is given as followed.

The overpotential $\eta$ / V observed in the experiment can be given by

$$\eta / V = a + b \ln j + j R \qquad (1)$$

where $a$ / V is the Tafel constant, $b$ / V dec$^{-1}$ is the Tafel slope, $j$ / A cm$^{-2}$ is the current density and $R/\Omega.cm^{-2}$ is the total area-specific uncompensated resistance of the system, which is assumed to be constant.

The derivative of equation (1) for current density gives equation (2) from which b and R can be easily obtained by plotting d$\eta$ / d$j$ as a function of $1/ j$

$$\frac{d\eta}{dj} = \frac{b}{j} + R \qquad (2)$$

The estimation of R allows correcting the experimental overpotential by subtracting the ohmic drop $jR$ according to equation (3).

$$\eta_{corr} = \eta - j R \qquad (3)$$

where $\eta_{corr}$ stands for the corrected overpotential

During the calculations, the derivatives d$\eta$ / d$j$ was replaced by their finite elements $\Delta\eta$ / $\Delta j$ estimated from each pair of consecutive experimental points.

## 3. Results and Discussion

### 3.1. Physical characterization of the electrodes

In Figure 1, the micrographs of the prepared electrodes were presented. It appears that the deposit has covered the surface. The surface of the $IrO_2$/Ti and $RuO_2$/Ti electrodes is rough with a mud cracked structure. That observation is similar to that is generally observed for thermally prepared $RuO_2$/Ti and $IrO_2$/Ti electrode [33-35]. Pores are also present on the deposit. The cracks observed on the electrodes surfaces occur during the cooling of the deposit because of the thermal shock to which these deposits are subjected during their retreat from the furnace.
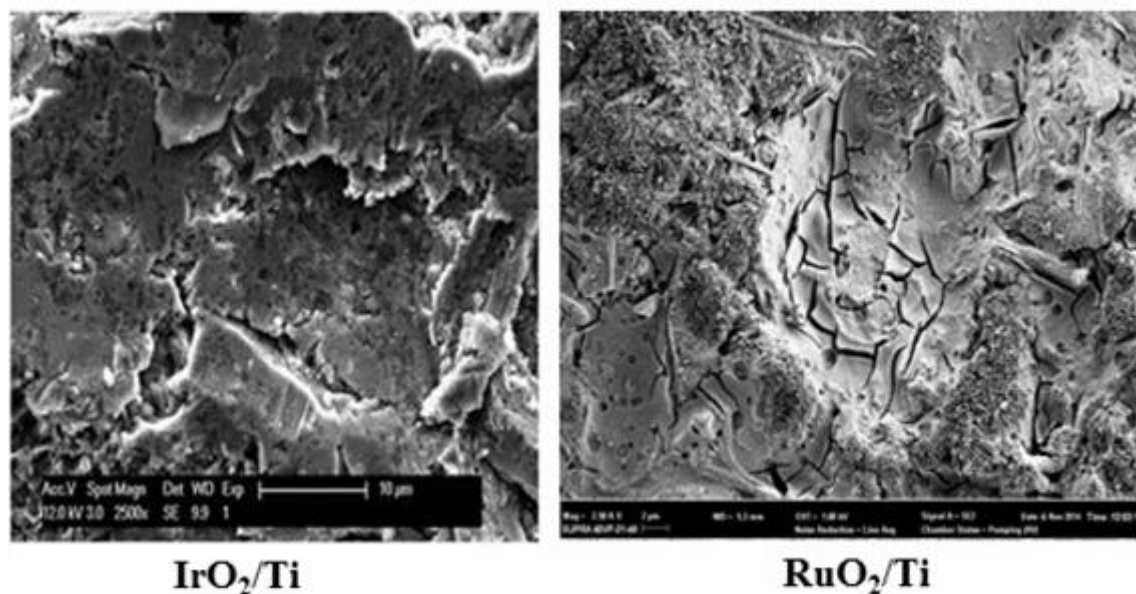
**Figure 1**. Scanning electron micrographs of IrO$_2$/Ti and RuO$_2$/Ti electrodes

### 3.2. Electrochemical characterization of the electrodes in acid media and acid media containing chloride

In Figure 2a, the voltammogram of the IrO$_2$ electrode recorded in 1 M HClO$_4$ at 100 mV/s was presented. A high voltammetric charge is observed with localized peaks at 0.7 and 1 V vs. SCE. These reversible broad peak characteristics of the redox transition of Ir(III)/Ir(IV) and Ir(IV)/Ir(VI) [36-40]. The capacitive load decreases for potentials lower than 0 V vs. SCE, indicating the electrode's low conductivity in this potential domain. One note an absence of surface redox process in the potential field. This result could be due to the strong resistance of the electrode in the potential cathodic [41]. The oxygen evolution reaction started around 1.23 V vs. SCE, with a rapid increase in the current. The voltammogram examen carried out at 100 mV/s in perchloric acid media revealed a quasi-symmetrical appearance in the potential explored [42].

The ratio of voltammetric charges | q (+) / q (-) | was calculated from the measurements carried out in 1 M HClO$_4$ media for different values of the scan rate presented in Figure 2b. This report shows that the cathode charge is greater than the anode charge at low potential scan rates. This result would indicate that at low potential scan rates, probably irreversible (slow) processes at the electrode have not been fully recovered during anodic scanning. On the other hand, for the high scan rate, whatever the potential scan rate, the cathodic charge is practically equal to the anode charge. Therefore, the curves are symmetrical throughout the potential domain regardless of the high scan rates' potential scan rate. This result shows that the observed anodic and cathodic peaks are related and can be attributed to the formation and reduction of the higher oxide (IrO$_3$) [43].
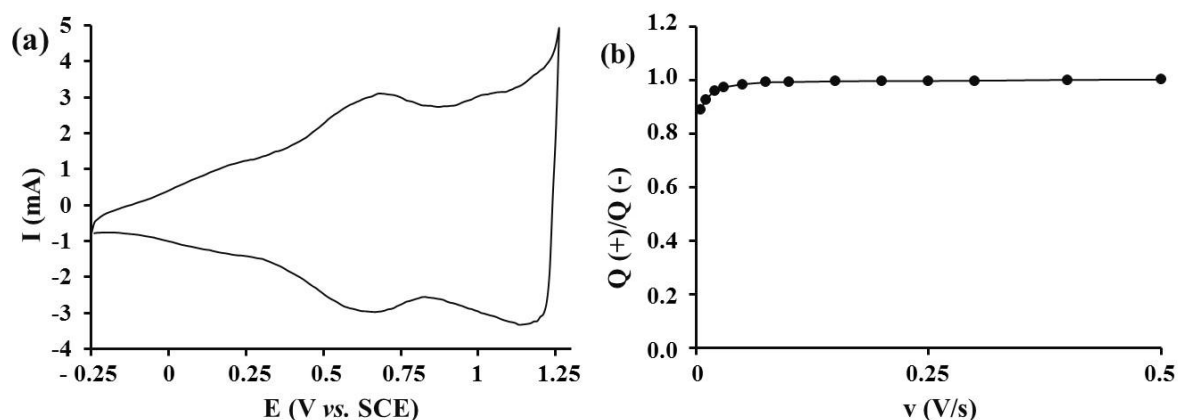


**Figure 2. (a)** Cyclic voltammogram recorded on IrO$_2$/Ti electrode in 1 M HClO$_4$ at 100 mV/s; **(b)** The ratio of voltammetric charges |q (+) / q (-)| according to the scan rate

Voltammetric measurements were performed in perchloric acid containing various concentrations of

NaCl on IrO$_2$ electrode. Figure 3 shows the different linear voltammograms obtained. This figure shows a

rapid increase in current intensity between 1.13 and 1.35 V vs. SCE, followed by another rapid growth in current from 1.35 V vs. SCE. The first increase in intensity would correspond to chloride oxidation to chlorine because the current intensity increases with chloride concentration. The chlorine evolution reaction starts at a lower potential than the oxygen evolution reaction obtained in the presence of $HClO_4$. This result shows the chlorine evolution reaction before the oxygen evolution reaction on this electrode.
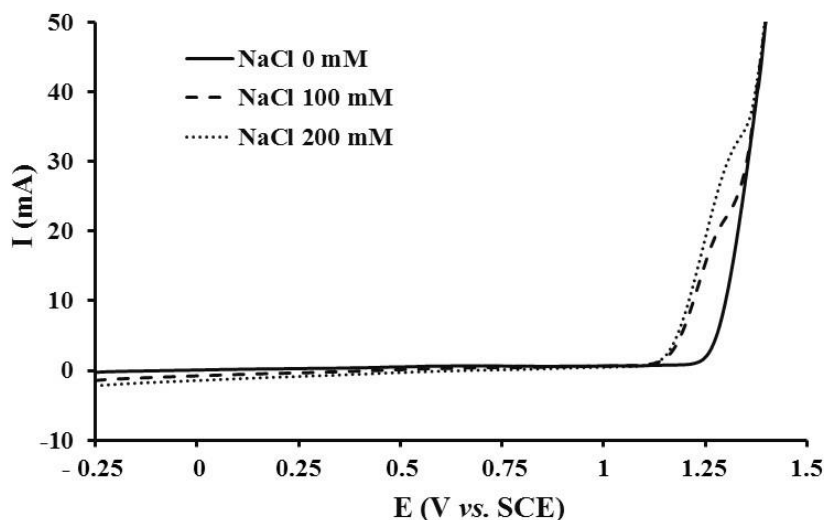


**Figure 3**. Linear voltammograms recorded on $IrO_2$/Ti electrode in 1 M $HClO_4$ containing NaCl at 100 mV/s

In Figure 4a, the voltammogram of the ruthenium dioxide electrode recorded in 1 M $HClO_4$ at 100 mV/s was presented. A rectangular shape voltammogram is observed with waves at 0.6 and 0.9 V vs. SCE. The presence of these waves could be due respectively to the redox transitions of Ru (III) / Ru (IV) and Ru (IV) / Ru (VI) on $RuO_2$ electrode surface [28]. This voltammogram is identical to that obtained in our previous work with the $RuO_2$ electrode [28]. This result confirms the presence of $RuO_2$ on our electrode. On this electrode, the oxygen evolution reaction starts at 1.2 V vs. SCE.

Figure 4b shows the $RuO_2$ voltammograms in 1 M $HClO_4$ containing chloride. A rapid increase of the current intensity is observed after 1.15 V vs. SCE for the concentrations investigated. This potential is lower than that of oxygen evolution. Then this rapid increase of the current would be related to the $Cl^-$ oxidation in $Cl_2$. Figure 5 shows the characteristics of $RuO_2$ electrode in the presence of $Cl^-$ only with the correction of the baseline linked to the supporting electrolyte. Oxidation peaks are observed. These peaks are $Cl^-$ to $Cl_2$ oxidation peaks because they increase with the $Cl^-$ concentrations. This result confirms that the rapid increase in current intensity observed from 1.15 V vs. SCE is related to the $Cl_2$ evolution reaction.
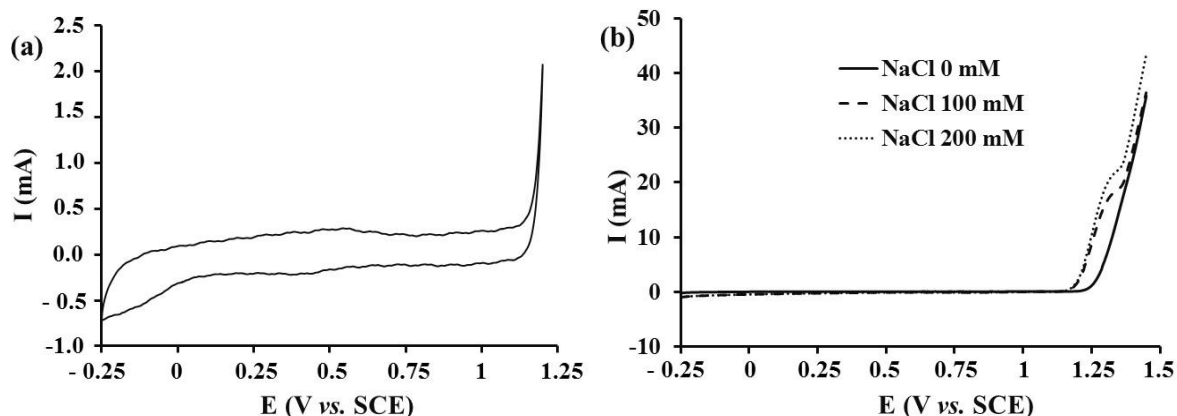


**Figure 4. (a)** Cyclic voltammogram recorded on $RuO_2$/Ti electrode in 1 M $HClO_4$ at 100 mV/s; **(b)** linear voltammograms recorded on $RuO_2$/Ti electrode in 1 M $HClO_4$ containing NaCl at 100 mV/s
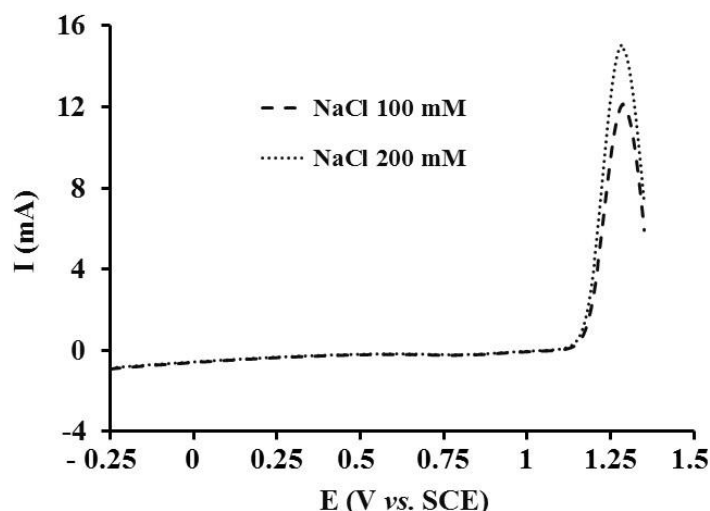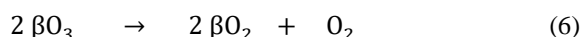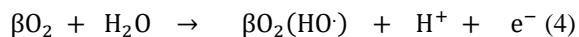
**Figure 5**. Linear voltammograms recorded on $RuO_2$/Ti electrode in NaCl with baseline correction related to the supporting electrolyte at 100 mV/s

From the obtained voltammograms, the Tafel slopes for the oxygen evolution reaction were determined. 39 and 40 mV/dec were obtained respectively for $IrO_2$ and $RuO_2$. This result shows that the prepared electrodes have the same oxygen evolution reaction kinetics in an acidic electrolyte. Taking into account these values of the Tafel slopes, obtained voltammograms and our previous work [24-26] and the literature [44,45] the following mechanism is proposed for the oxygen evolution reaction in acid media on our electrodes:

$$\beta O_2 + H_2O \rightarrow \beta O_2(HO^{.}) + H^+ + e^- \quad (4)$$

$$\beta O_2(HO^{.}) \rightarrow \beta O_3 + H^+ + e^- \quad (5)$$

$$2\,\beta O_3 \rightarrow 2\,\beta O_2 + O_2 \quad (6)$$

Where $\beta$ is Ir or Ru

The mechanism described by eqs. (4-6) predicts the Tafel slope of 120 mV/dec if the first step is represented by eq. (4) the rate-determining step (rds), 40 mV/dec if the second step is described by eq. (5) rds and 30 mV/dec if the third step is represented by eq. (6) is rds. For OER on $IrO_2$ or $RuO_2$ in $HClO_4$ medium, the rate-determining step is the step described by eq. (5), because the Tafel slope is 40 mV/dec.

The Tafel slopes were also determined for the chlorine evolution reaction in acidic media. 40 mV/ dec was obtained with $IrO_2$ and $RuO_2$ electrodes. This result shows that these electrodes have the same kinetic of the chlorine evolution reaction in acidic media. According to our previous work [25,28,] and the Tafel slopes value, a global chlorine evolution reaction mechanism is described as followed in acidic media. After the formation of higher oxides ($\beta O_3$) in the eq.5, chloride ions attach themselves to the higher degree oxide (eq. 7), then chlorine is produced (eq. 8).

$$\beta O_3 + Cl^- \rightarrow \beta O_3(Cl) + e^- \quad (7)$$

$$\beta O_3(Cl) + H^+ + Cl^- \rightarrow \beta O_2(HO^{.}) + Cl_2 \quad (8)$$
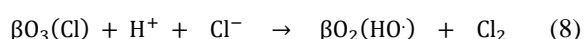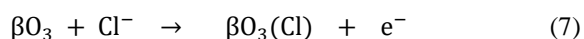
Where $\beta$ is Ir or Ru

This mechanism predicts the following Tafel slopes: 120 mV/dec if the first step (eq. 5) is the rate-determining step (rds), 40 mV/dec for the second step (eq. 7), and 30 mV/dec for the third step (eq. 8). For chlorine evolution reaction on $IrO_2$ or $RuO_2$ in $HClO_4$ medium, the rate-determining step is described by eq. (7), because the Tafel slope is 40 mV/dec.

**3.3. Formic acid oxidation without chloride**

Figure 6a shows the voltammograms recorded on $IrO_2$ in formic acid media. No peak characteristic of the formic acid oxidation for the potential domain between - 0.25 and 1 V vs. SCE is observed when an organic compound is added to these voltammograms. This result indicates that $IrO_2$ electrode is not electrocatalytic for HCOOH oxidation on this domain. After 1 V vs. SCE, a modification is observed on the voltammograms. The current intensity increases as the organic compound concentration increase for a given potential. The oxygen evolution potential decreases with the rise of the formic acid concentration. In the absence of formic acid, the oxygen evolution starts at 1.22 V vs. SCE. In the presence of formic acid, the oxygen evolution starts at 1.1 V vs. SCE for a formic acid concentration of 0.5 M and 1.04 V vs. SCE for 1 M.

In order to determine the behavior of $IrO_2$ in a formic acid media with correction of the baseline linked to the support electrolyte, the curves of Figure 6b were carried out. To get it, the current intensities obtained in the absence of formic acid were subtracted from the current intensities obtained in the presence of formic acid. This subtraction makes it possible to get the current linked to the organic compound oxidation. From - 0.25 to 1 V vs. SCE, no oxidation peak of formic acid is observed. There is a rapid increase in current after 1 V vs. SCE. We observe a shift of the curve to the left when the concentration of formic acid increases. The current intensity increases with the rise

of formic acid concentration. The rapid increase after 1 V vs. SCE would be related to the formic acid oxidation in which the species from the

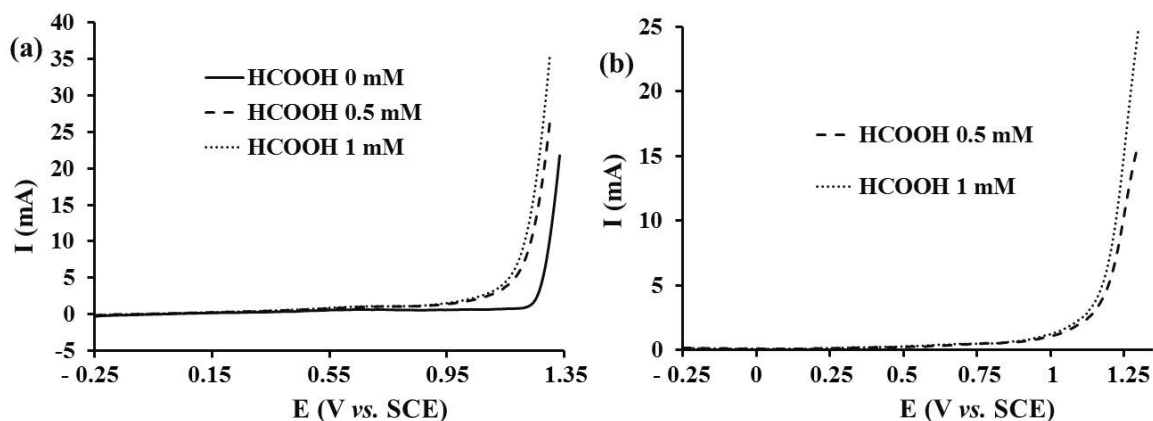electrochemical decomposition of water are likely to intervene.



**Figure 6. (a)** linear voltammograms of HCOOH oxidation on IrO$_2$/Ti electrode; **(b)** IrO$_2$/Ti electrode in a formic acid with the baseline linked to the electrolyte support at 20 mV/s

HCOOH oxidation on ruthenium oxide is shown in Figure 7a. This figure shows that the voltammetric curves change recorded in the absence and then in formic acid are observed at potentials higher than 1 V vs. SCE. From -0.25 to 1 V vs. SCE, these voltammograms are almost superimposable. No peak characteristic of formic acid oxidation is observed in this potential domain. On the other hand, there is a shift in the oxygen evolution reaction potential to the left as the amount of formic acid increases. For 0; 0.5 and 1 mM of formic acid, the oxygen evolution reaction start respectively at 1.17; 1.05 and 1.01 V vs. SCE. The current intensity increases with the increase of formic acid concentration. For a potential of 1.17 V vs. SCE, the current intensity is 0.24 mA in the absence of formic acid. In the presence of 0.5 and 1 mM formic acid, the current intensities are 0.99 mA and 1.68 mA, respectively.

Figure 7b shows the characteristics of RuO$_2$ in a formic acid media with correction of the baseline linked to the support electrolyte. In this figure, oxidation peaks are observed whose intensity increases with the increase of formic acid concentration. This result shows that the observed peaks reflect the organic compound oxidation and confirms the previous observations. Our observations have shown that the formic acid oxidation on IrO$_2$ or RuO$_2$ occurs at high potentials with a simultaneous oxygen evolution reaction. In what follows, we propose a global mechanism of the response on the surface of the electrodes. For this result, we assume that the active species of the higher oxides (IrO$_3$ or RuO$_3$) are involved in the oxidation process. In this mechanism, the organic compound oxidation occurs on the surface of IrO$_2$ or RuO$_2$. The higher oxides are also involved in the oxygen evolution reaction.
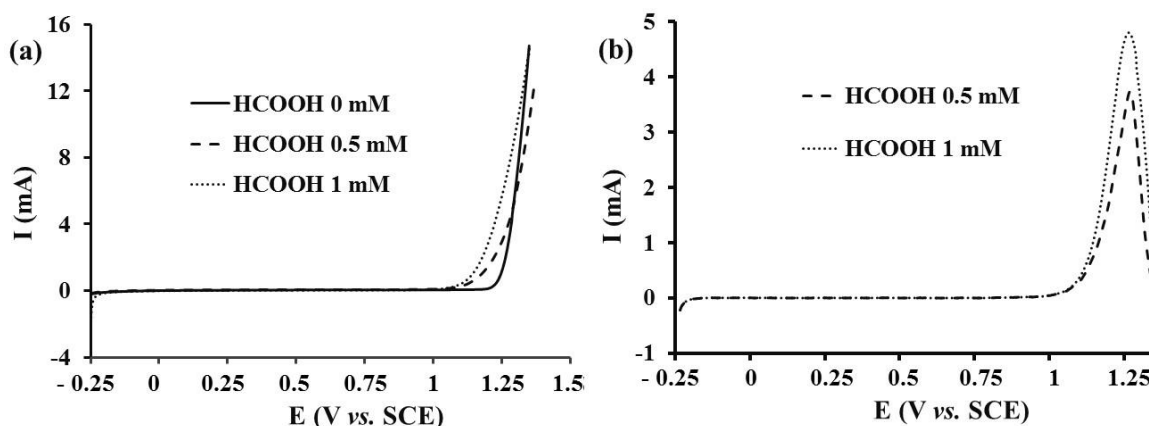


**Figure 7. (a)** linear voltammograms of HCOOH oxidation on RuO$_2$/Ti electrode; **(b)** RuO$_2$/Ti electrode in a formic acid with the baseline linked to the electrolyte support at 20 mV/s

Indeed, it follows from the previous observations that the organic compound oxidation occurs after 1 V vs. SCE in a domain where the voltammetric measurements had revealed the redox transitions Ir (IV) / Ir (VI) IrO$_2$ / IrO$_3$ with IrO$_2$ electrode. With

RuO$_2$, the Ru (IV) / Ru (VI) redox transitions are observed in the same potential domain. These observations made it possible to propose the following mechanism for the organic compound

oxidation and the simultaneous oxygen evolution reaction in an acid media without chloride.

During the formic acid oxidation, the first reaction is the electrochemical decomposition of water molecules, leading to hydroxyl radicals [46]. These hydroxyl radicals resulting from the electrochemical decomposition of water are instantly adsorbed on the electrode surface. Since iridium oxide and ruthenium oxide are active electrodes, there is a strong interaction between the electrode and the hydroxyl radicals. In this case, the adsorbed hydroxyl radicals can interact with the anode followed by a redox transition at the electrode surface, forming a higher oxide ($IrO_3$ or $RuO_3$). $IrO_3$ or $RuO_3$ can act as a mediator in the organic compounds (eq. 9). This organic compound oxidation reaction competes with the oxygen evolution reaction eq. 6.

$$\beta O_3 + HCOOH \rightarrow \beta O_2 + CO_2 + H_2O \quad (9)$$
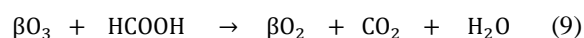
### 3.4. Formic acid oxidation in acid media containing chloride

The formic acid oxidation in an acid media containing chloride on the $IrO_2$ electrode is shown in Figure 8. This figure's voltammograms show that no significant change is observed at - 0.25 to 1 V vs. SCE when the organic compound is added. By exploring high potential domains from 1.1 to 1.4 V vs. SCE, it is noted that the current increases when HCOOH is added to the electrolytic solution. The anode wave observed at 1.27 V vs. SCE in the absence of HCOOH is almost invisible in the presence of HCOOH. In the presence of formic acid, the current increases rapidly after the wave at 1.27 V vs. SCE. Chloride would therefore intervene indirectly in the HCOOH oxidation.

In the presence of chloride, Figure 9 shows the voltammograms recorded on ruthenium oxide. The voltammograms show an oxidation peak at 1.29 V vs. SCE. These peaks could be due to the chloride oxidation in the electrolyte. The intensity of the oxidation peak increases with the increase of formic acid concentration while the reduction peak remains constant. The increase in the oxidation intensity wave would be characteristic of the organic compound oxidation. This oxidation probably occurs consecutively to that of the chloride [47]. Then in the presence of Cl⁻, the HCOOH oxidation on these electrodes would proceed according to the following mechanism:
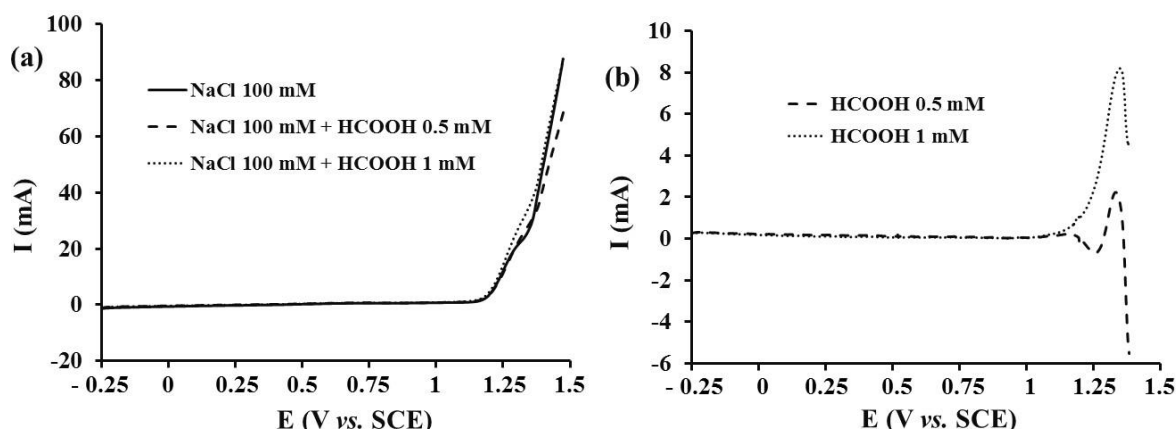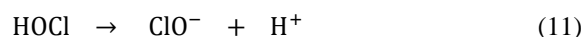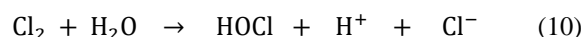
$$Cl_2 + H_2O \rightarrow HOCl + H^+ + Cl^- \quad (10)$$

$$HOCl \rightarrow ClO^- + H^+ \quad (11)$$

$$HCOOH + ClO^- \rightarrow CO_2 + H_2O + Cl^- \quad (12)$$



**Figure 8. (a)** Formic acid oxidation in acid media containing 0.1 M chloride on $IrO_2$/Ti electrode; **(b)** $IrO_2$/Ti electrode in a formic acid with the baseline linked to the electrolyte support at 20 mV/s
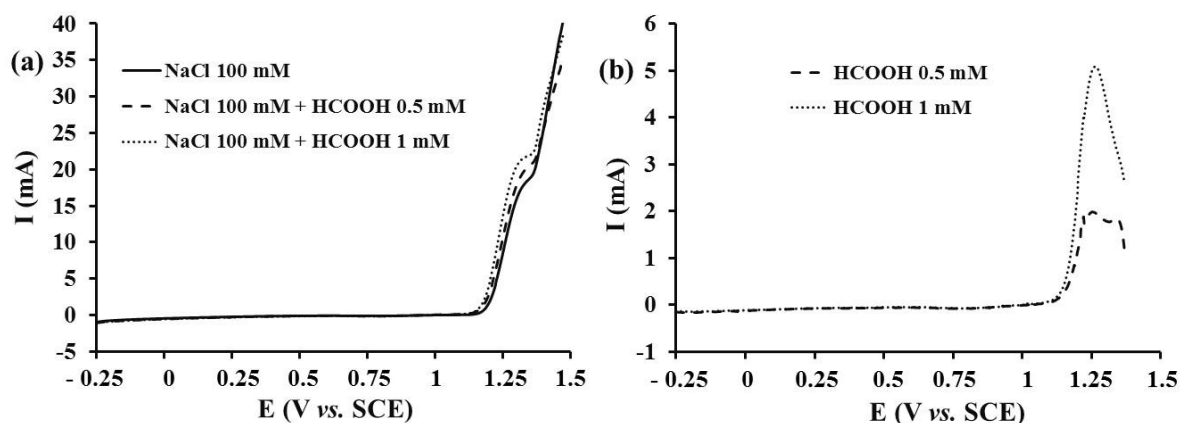


**Figure 9. (a)** Formic acid oxidation in acid media containing 0.1 M chloride on $RuO_2$/Ti electrode; **(b)** $RuO_2$/Ti electrode in a formic acid with the baseline linked to the electrolyte support at 20 mV/s

There is, therefore, a first step, which consists of chloride oxidation. This leads to the chlorine evolvement on the different electrodes. The formed chlorine is then hydrolyzed to hypochlorous acid (HOCl), which is a powerful oxidant. In acidic media, hypochlorous acid releases its proton ($H^+$) and forms the hypochlorite ion ($ClO^-$). It is these ions ($ClO^-$) that oxidize the organic compound [47].
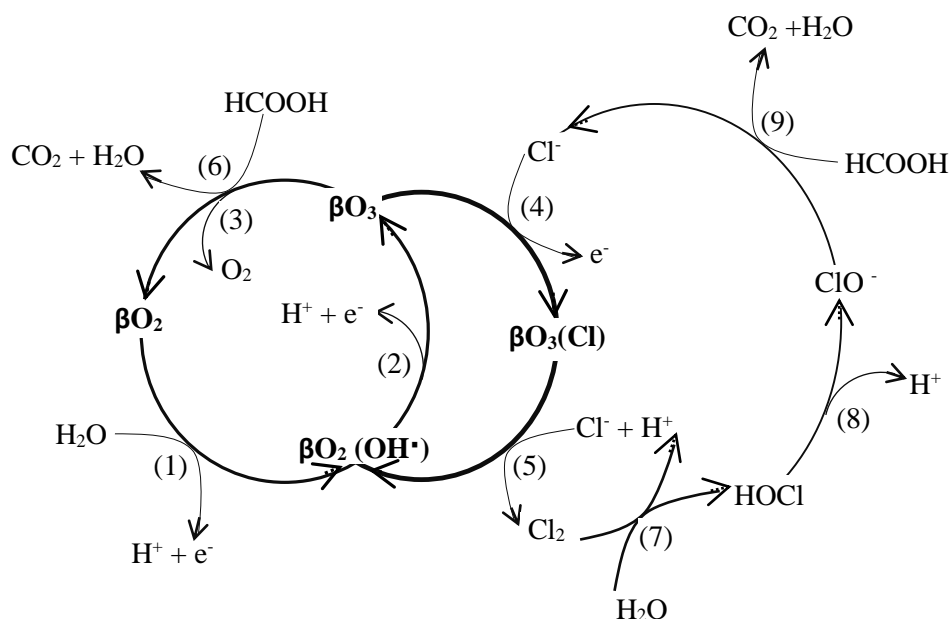


**Figure 10.** Mechanisms of formic acid oxidation in the presence of oxygen evolution and chlorine evolution

By relying on the mechanisms of oxygen evolution reaction, chlorine evolution reaction, and formic acid oxidation above, Figure 10 makes it possible to propose a mechanism for the formic acid oxidation in acid media contains chloride. Concerning the oxygen evolution in acid media, we have steps 1, 2, and 3. In acid media containing $Cl^-$, $Cl^-$ is fixed on the higher oxide, then the chlorine occurs, and the adsorbed radical is regenerated (steps 4 and 5). In the presence of HCOOH, the higher oxide ($IrO_3$ or $RuO_3$) allows the organic compound oxidation to $CO_2$ and $H_2O$ (step 6). This organic compound oxidation reaction competes with the oxygen evolution reaction (steps 3 and 6).

In acid media containing chloride, the oxidation mechanism of organic compounds is complex. The chlorine produced indirectly intervenes in the organic compound oxidation according to steps 7, 8, and 9 of the mechanism. The chlorine makes it possible to oxidize HCOOH and regenerates $Cl^-$. In the presence of chloride, the HCOOH oxidation on the $IrO_2$ and $RuO_2$ electrodes takes place at high potentials. At high potentials, the $Cl^-$ oxidation leads to the production of $Cl_2$ or $ClO^-$. Thus, the formic acid oxidation occurs indirectly via hypochlorite ions and directly on the electrodes' active sites in competition with the oxygen evolution reaction.

**4. Conclusion**

The physical and electrochemical characterizations performed on these electrodes revealed the presence of $IrO_2$ or $RuO_2$. This work has shown that $RuO_2$ and $IrO_2$ have the same kinetics of oxygen evolution and

chlorine evolution. The voltammograms obtained made it possible to show that the prepared metal oxide electrodes could oxidize the organic compounds. However, the oxidation current of the organic compound increases in the presence of chloride. In HCOOH, the higher oxide ($IrO_3$ or $RuO_3$) acts as a mediator in the oxidation of the organic compounds in competition with the oxygen evolution reaction. In acid media containing chloride, the oxidation mechanism of organic compounds is complex. At high potentials, the oxidation of $Cl^-$ leads to the production of $Cl_2$. This reaction competes with the oxygen evolution reaction and the reaction's formic acid oxidation reaction via hydroxyl radicals. The chlorine produced is transformed into a hypochlorite ion, which is involved in the formic acid oxidation.

**References**

1- C.A. Martínez-Huitle, E. Brillas, Decontamination of wastewaters containing synthetic organic dyes by electrochemical methods: A general review, Appl. Catal. B Environ., **2009**, 87, 105–145.

2- C.A. Martinez-Huitle, S. Ferro, Electrochemical oxidation of organic pollutants for the wastewater treatment: direct and indirect processes, Chem. Soc. Rev., **2006**, 35, 1324–1340.

3- M. Panizza, G. Cerisola, Direct and mediated anodic oxidation of organic pollutants, Chem. Rev., **2009**, 109, 6541–6569.

4- C.A. Martinez-Huitle, E. Brillas, Angew, Electrochemical alternatives for drinking water

disinfection, Angew Chem. Int. Ed., **2008**, 47, 1998–2005.

5- E. Brillas, I. Sirés, M.A. Oturan, Electro-Fenton process and related electrochemical technologies based on Fenton's reaction chemistry, Chem. Rev., **2009**, 109, 6570–6631.

6- I. Sirés, E. Brillas, M.A. Oturan, M.A. Rodrigo, M. Panizza, Electrochemical advanced oxidation processes: today and tomorrow. A review, Environ. Sci. Pollut. Res., **2014**, 21, 8336–8367.

7- J.H.B. Rocha, A.M.S. Solano, N.S. Fernandes, D.R. da Silva, J.M. Peralta-Hernandez, C.A. Martínez-Huitle, Electrochemical Degradation of Remazol Red BR and Novacron Blue C-D Dyes Using Diamond Electrode, Electrocatalysis, **2012**, 3, 1–12.

8- J.L. Nava, M.A. Quiroz, C.A. Martínez-Huitle, Electrochemical Treatment of Synthetic Wastewaters Containing Alphazurine A Dye: Role of Electrode Material in the Colour and COD Removal, J. Mexican Chem. Soc., **2008**, 52, 249–255.

9- D. Shao, W. Lyu, J. Cui, X. Zhang, Y. Zhang, G. Tan, W. Yan, Polyaniline nanoparticles magnetically coated Ti/Sb–SnO$_2$ electrode as a flexible and efficient electrocatalyst for boosted electrooxidation of biorefractory wastewater, Chemosphere, **2020**, 241, 125103.

10- C. Ridruejo, C. Salazar, P.L. Cabot, F. Centellas, E. Brillas, I. Sires, Electrochemical oxidation of anesthetic tetracaine in aqueous medium. Influence of the anode and matrix composition, Chem. Eng. J., **2017**, 326, 811–819.

11- S. Ghasemian, S. Omanovic, Fabrication, and characterization of photoelectrochemically-active Sb-doped Snx-W(100–x) %-oxide anodes: towards the removal of organic pollutants from wastewater, Appl. Surf. Sci., **2017**, 416, 318–328.

12- X. Li, H. Xu, W. Yan, Fabrication and characterization of PbO$_2$ electrode modified with polyvinylidene fluoride (PVDF), Appl. Surf. Sci., **2016**, 389, 278–286.

13- P. Duby, The history of progress in dimensionally stable anodes, JOM, **1993**, 45, 41–43.

14- L.A.G. Pohan, O. Kambiré, M. Berté, L. Ouattara, Study of lifetime of Platinum Modified Metal Oxides Electrodes, Int. J. Biol. Chem. Sci., **2020**, 14, 1479-1488.

15- S. Trasatti, Electrocatalysis: understanding the success of DSA®, Electrochimica Acta, **2000**, 45, 2377-2385.

16- D. Rajkumar, J. Guk Kim, K. Palanivelu, Indirect electrochemical oxidation of phenol in the presence of chloride for wastewater treatment, Chemical engineering & technology, **2005**, 28, 98-105.

17- M.B. Gawande, R.K. Pandey, R.V. Jayaram, Role of mixed metal oxides in catalysis science— versatile applications in organic synthesis, Catal. Sci. Technol., **2012**, 2, 1113.

18- G. Wang, L. Zhang, J. Zhang, A review of electrode materials for electrochemical Supercapacitors, Chem. Soc. Rev., **2012**, 41, 797–828.

19- F.L. Souza, M. Aquino, D.W. Miwa, M.A. Rodrigo, A.J. Motheo, Photo-assisted electrochemical degradation of the dimethyl phthalate Ester on DSA®. Electrode, J. Environ. Chem. Eng., **2014**, 2, 811–818.

20- R. Pelegrini, P.P. Zamora, A.R. De Andrade, J. Reyes, N. Dura'n, Electrochemically assisted photocatalytic degradation of reactive dyes, Appl. Catal. B, **1999**, 22, 83–90.

21- G. Li, M. Zhu, J. Chen, Y. Li, X. Zhang, Production and contribution of hydroxyl radicals between the DSA anode and water interface, J. Environ. Sci., **2011**, 23, 744–748.

22- D. Traore, A.S.M. abdelaziz, Y.S. Brou, A. Trokourey, Determination of Cu$^{2+}$ by N, N-dichromone-p-phenylenediamine modified carbon paste electrode, Int. J. Biol. Chem. Sci., **2014**, 8, 2773-2785.

23- K.M. Koffi, L. Ouattara, Electroanalytical Investigation on Paracetamol on Boron-Doped Diamond Electrode by Voltammetry, American Journal of Analytical Chemistry, **2019**, 10, 562-578

24- O. Kambire, L.A.G. Pohan, F.T.A. Appia, C.Q.M. Gnamba, K.H. Kondro, L. Ouattara, Influence of various metallic oxides on the kinetic of the oxygen evolution reaction on platinum electrodes, J. Electrochem. Sci. Eng., **2015**, 5, 79-91.

25- O. Kambire, L.A.G. Pohan, F.T.A. Appia, L. Ouattara, Anodic Oxidation of Chlorides on Platinum Modified by Metallic Oxides, Int. J. Pure Appl. Sci. Technol., **2015**, 27, 27-43.

26- O. Kambiré, L.A.G. Pohan, K.H. Kondro, L. Ouattara, Study of oxygen evolution reaction on thermally prepared xPtO$_{y-(100-x)}$IrO$_2$ electrodes, J. Electrochem. Sci. Eng., **2020**, 10, 347-360.

27- Y. Kang, C.B. Murray, Formic Acid Oxidation. Encyclopedia of Applied Electrochemistry, **2014**, 895-901.

28- O. Kambire, F.T.A. Appia, L. Ouattara, Oxygen and chlorine evolution on ruthenium dioxide modified by platinum in acid solutions, Rev. Ivoir. Sci. Technol., **2015**, 25, 21-33.

29- A. Kapalka, G. Fóti, C. Comninellis, Determination of the Tafel slope for oxygen evolution on boron-doped diamond electrodes, Electrochemistry Communications, **2008**, 10, 607-610.

30- G. Rocchini, The influence of the ohmic drop on the shape of polarization curves, Corrosion Science, **1993**, 34, 2019-2030.

31- L.A. De Faria, J.F.C. Boodts, S. Trasatti, Electrocatalytic properties of ternary oxide mixtures of composition Ru$_{0.3}$Ti$_{(0.7-x)}$Ce$_x$O$_z$: oxygen evolution from acidic solution, Journal of Applied Electrochemistry, **1996**, 26, 1195-1199.

32- N. Krstajic, S. Trasatti, Cathodic behaviour of $RuO_2$-doped $Ni/Co_3O_4$ electrodes in alkaline solutions: hydrogen evolution, Journal of Applied Electrochemistry, **1998**, 28, 1291-1297.

33- F.T.A. Appia, C.Q.M. Gnamba, O. Kambiré, M. Berté, S.P. Sadia Sahi placide, I. Sanogo, L. Ouattara, Electrochemical Oxidation of Amoxicillin in Its Commercial Formulation on Thermally Prepared $RuO_2/Ti$, J. Electrochem. Sci. Technol., **2016**, 7, 82-89.

34- M. Berté, F.T.A. Appia, I. Sanogo, L. Ouattara, Electrochemical Oxidation of the Paracetamol in its Commercial Formulation on Platinum and Ruthenium Dioxide Electrodes, Int. J. Electrochem. Sci., **2016**, 11, 7736–7749

35- K.H. Kondro, L. Ouattara, A. Trokourey, Y. Bokra, Investigation of the electrochemical behaviour of thermally prepared $Pt-IrO_2$ electrodes, Bull. Chem. Soc. Ethiop., **2008**, 22, 125-134.

36- T.C. Wen, C.C. Hu, Hydrogen and Oxygen Evolutions on Ru-Ir Binary Oxides Journal of Electrochem. Soc., **1992**, 139, 2158-2163.

37- V.A. Alves, L.A. Da Silva, J.F.C. Boodts, Surface characterization of $IrO_2/TiO_2/CeO_2$ oxide electrodes and Faradaic impedance investigation of the oxygen evolution reaction from alkaline solution, Electrochimica Acta., **1998**, 44, 1525-1534.

38- H. Chen, S. Trasatti, Cathodic behavior of $IrO_2$ electrodes in alkaline solution: Part 2. Kinetics and electrocatalysis of $H_2$ evolution, Journal of Electroanalytical Chemistry, **1993**, 357, 91-103.

39- G. Foti, C. Mousty, V. Reid, C. Comninellis, Characterization of DSA type electrodes prepared by rapid thermal decomposition of the metal precursor, Electrochimica Acta., **1998**, 44, 813-818.

40- C. Mousty, G. Fóti, C. Comninellis, V. Reid, Electrochemical behavior of DSA type electrodes prepared by induction heating, Electrochimica Acta., **1999**, 45, 451-456.

41- V.V. Panic, A.B. Dekanski, M. Mitrić, S.K. Milonjić, V.B. Misković-Stanković, B.Z. Nikolić, The effect of the addition of colloidal iridium oxide into sol-gel obtained titanium and ruthenium oxide coatings on titanium on their electrochemical properties, Phys. Chem. Chem. Phys., **2010**, 12, 7521–7528.

42- S. Fierro, A. Kapałka, C. Comninellis, Electrochemical comparison between $IrO_2$ prepared by thermal treatment of iridium metal and $IrO_2$ prepared by thermal decomposition of $H_2IrCl_6$ solution, Electrochemistry Communications, **2010**, 12, 172–174

43- S. Fierro, L. Ouattara, E.H. Calderon, E. Passas-Lagos, H. Baltruschat, C. Comninellis, Investigation of formic acid oxidation on $Ti/IrO_2$ electrodes, Electrochimica Acta., **2009**, 54, 2053–2061

44- L. Ouattara, S. Fierro, O. Frey, M. Koudelka, C. Comninellis, Electrochemical comparison of $IrO_2$ prepared by anodic oxidation of pure iridium and $IrO_2$ prepared by thermal decomposition of $H_2IrCl_6$ precursor solution, J Appl Electrochem, **2009**, 39, 1361–1367.

45- N. Yuan, Q. Jiang, J. Li, J. Tan, A review on non-noble metal-based electrocatalysis for the oxygen evolution reaction, Arabian Journal of Chemistry, **2020**, 13, 4294-4309.

46- M.T. Fukunaga, J.R. Guimarães, R. Bertazzoli, Kinetics of the oxidation of formaldehyde in a flow electrochemical reactor with $TiO_2/RuO_2$ anode, Chemical Engineering Journal, **2008**, 136, 236–241.

47- A.L.G. Pohan, L. Ouattara, K.H. Kondro, O. Kambiré, A. Trokourey, Electrochemical Treatment of the Wastewaters of Abidjan on Thermally Prepared Platinum Modified Metal Oxides Electrodes, European Journal of Scientific Research, **2013**, 94, 96-108.